J Electroceram (2009) 23:94–101
DOI 10.1007/s10832-008-9546-7

Pyroelectric and dielectric properties of lead lanthanum zirconate titanate $(Pb_{0.92}La_{0.08})(Zr_{0.65}Ti_{0.35})O_3$-P(VDF/TFE) (0.98/0.02) nanocomposites

Marian Olszowy · Ewa Markiewicz · Czesław Pawlaczyk · Jan Kułek · Ewa Nogas-Ćwikiel

Received: 28 September 2007 / Accepted: 8 August 2008 / Published online: 28 August 2008

Abstract PLZT-P(VDF/TFE) 0–3 composites with nanosized lead lanthanum zirconate titanate $(Pb_{0.92}La_{0.08})(Zr_{0.65}Ti_{0.35})O_3$ (PLZT 8/65/35) ceramic powders of volume fraction Φ up to 0.2 were fabricated using PLZT powders imbedded in a copolymer P(VDF/TFE)(0.98/0.02) matrix. The PLZT nanopowders were prepared by the sol-gel technique. The PLZT-P(VDF/TFE) composite samples were prepared from ceramic and polymer powders by the hot-pressing method. Dielectric response was studied in the frequency range from 100 Hz to 1 MHz and at temperatures from 100 to 450 K. The pyroelectric properties were studied by dynamic method with modulation frequency from 1 to 100 Hz. The dielectric response of the ceramics-polymer composite was found to be a combination of the responses of the pure polymer and the ceramics: (1) the addition of the PLZT ceramics increases the value of the dielectric permittivity ε', (2) the composite shows the maximum of the permittivity coming from the PLZT ceramics, (3) the temperature dependences of the dielectric loss tgδ are characterized by the maximum attributed to the α-relaxation (glass transition) in the pure polymer. The pyroelectric coefficient of the composite increases from ~20 $\mu C/m^2K$ in pure P(VDF/TFE) to ~140 $\mu C/m^2K$ in the composites of Φ=0.15.

Keywords Dielectric relaxation · Pyroelectric properties · PLZT · Nanocomposites

M. Olszowy (✉)
Institute of Physics, University of Zielona Góra,
4a Prof. Szafrana Str.,
65-516 Zielona Góra, Poland
e-mail: M.Olszowy@if.uz.zgora.pl

E. Markiewicz · C. Pawlaczyk · J. Kułek
Institute of Molecular Physics, Polish Academy of Sciences,
17 Smoluchowskiego Str.,
60-179 Poznań, Poland

E. Nogas-Ćwikiel
Faculty of Computer Science and Materials Science,
University of Silesia,
2 Śnieżna Str.,
41-200 Sosnowiec, Poland

1 Introduction

In recent years, ceramic-polymer composites containing ferroelectric ceramics dispersed in a polymer matrix have aroused increased interest due to their good mechanical flexibility, low dielectric loss, and excellent piezo- and pyroelectric properties [1–4]. Composites of 0–3 connectivity (a polymer phase three dimensionally connected with isolated ceramic particles) can be easily prepared in a form of flexible sheets. The properties of the composite depend on the properties of both components: on the one hand on the composition of the ceramics, its crystal structure and the microstructure morphology including grain size, grain boundaries, pores, crystallinity, micro-cracks, etc. [1], on the other hand the dynamic dielectric properties are determined first of all by the dielectric response of the polymer matrix [5]. Composites of nanometer-sized ferroelectric PLZT powders with copolymer originated from PVDF were found to exhibit electroactivity suitable for various applications at ambient temperature [4].

The lead lanthanum zirconate titanates (PLZT) ceramics have attracted considerable attention in recent years because they offer a broad range of dielectric, electromechanical and optical properties [6–9]. The majority of PLZT properties of are the function of the La concentration and so the Zr/Ti ratio. At a Zr/Ti ratio of 65/35 mol.%, PLZT displays a very high electromechanical coupling coefficient and stays ferroelectric up to a La content of about 10 at.%

at the room temperature. The powder material of PLZT *x*/65/35 ceramics used to produce PLZT-P(VDF/TFE) composites was containing 8 at.% La (*x*). PLZT 8/65/35 is characterized by high dielectric permittivity (3,400), high density (7.80 g/cm^3) and electromechanical coupling factor (0.65) [7] and exhibits rhombohedral symmetry. It has also been observed that PLZT has a diffuse phase transition and ferroelectric relaxor behaviour [10]. Pure P(VDF/TFE) (0.98/0.02) obtained by hot-pressing shows a relaxation processes related to the glass transition (~303 K) [11, 12].

The strong dependence of the dielectric spectrum of the PLZT ceramics on the lanthanum content [13] gives the possibility to design the composites with the dielectric properties matched to the practical requirements. The PLZT *x*/65/35 compounds with $7<x<12$ are known to exhibit classical relaxor behavior and are of great practical interest [14]. In our previous work [4] we studied the properties of nanocomposites of PLZT-9.5/65/35 ceramics and copolymer of vinylidene fluoride with trifluoroethylene—P(VDF/TrFE) (50/50). Moreover, the composites are known to show lower acoustic impedance matched to water and tissue. This property offers the possibility of application in electromechanical transducers, which have both the sensor and actuator functions. Better elastic properties of the composites give the possibility that they can be easily prepared in variety of shapes.

The subject of this paper are the dielectric and pyroelectric properties of composites made from copolymer of vinylidene fluoride with tetrafluoroethylene P(VDF/TFE)(0.98/0.02) loaded with PLZT-8/65/35 ceramics. This composition was aimed at lower dielectric losses of this new material which are required in pyroelectric sensors. In the present work we studied: (1) morphology and grain size distribution of PLZT 8/65/35 nanopowders; (2) microstructure and qualification of chemical composition of bulk ceramics; (3) dielectric response of a hot-pressed PLZT 8/65/35 ceramics, pure P(VDF/TFE)(0.98/0.02) polymer and PLZT-P(VDF/TFE) nanocomposites with the volume fraction of the ceramics Φ=0.1, 0.15 and 0.2 as a function of frequency and temperature; (4) pyroelectric properties of all of them at the room temperature. The relaxation characteristics of samples were also analyzed using the Vogel–Fulcher relation.

2 Experimental

The 0–3 nanocomposite reported in the paper were prepared by hot-pressing (3.2 MPa, 450 K, 10 min) of the powder mixture and cooled to the room temperature under pressure at a rate of 8 K/min. Lead lanthanum zirconate titanate $(Pb_{0.92}La_{0.08})(Zr_{0.65}Ti_{0.35})O_3$ (PLZT 8/65/35) powders were prepared by the sol-gel method. The sol-gel method is a low temperature process, which utilizes chemical precursors and makes it possible to obtain fine powders that exhibit better purity and homogeneity than those obtained by conventional high-temperature processes. Nanosized powders of PLZT 8/65/35 were synthesizes using: lead(II)acetate trihydrate, lanthanum acetate hydrate, zirconium(IV)propoxide and titanium(IV)propoxide. Powders obtained from dried gels were calcined at 873 K. The temperature was identified by thermogravimetric analysis (TGA) and 6 h was necessary to burn off organic remains. The P(VDF/TFE) copolymer powder of VDF mol contents x=0.98 was delivered by Nitrogeneous Concern (Tarnów, Poland). The PLZT-P(VDF/TFE) composite samples had the form of discs with a diameter of 11 mm, thickness of 80–220 μm and the volume fraction of the ceramics Φ amounted 0.1, 0.15 and 0.2. Bulk ceramics was prepared from PLZT 8/65/35 powders by the hot-pressing method at the temperature T_p=1473 K during 2 h under the pressure p=20 MPa. Gold electrodes were evaporated on both sides of the samples using a Baltec SCD 050 sputter coater. The morphology of powders and microstructure of ceramics were investigated by means of Hitachi S-4700 scanning electron microscope with Noran Vantage system of microanalysis used for the qualification of chemical composition of samples. The grain size distributions of PLZT nanopowders were estimated by the DLS method using Zetasizer Nano ZS.

The dielectric response was studied in the frequency range 100 Hz to 1 MHz using a computer aided HP 4284A LCR meter. The samples were mounted in the CF 1204 Oxford Instruments cryostat equipped with the ITC 4 temperature controller. The measurements were performed during heating from 100 to 450 K at a rate of 1 K/min.

Modified Chynoweth method [15] was used to study the pyroelectric response at the room temperature in the voltage mode with loading resistance of 1 GΩ. The samples were polarized in electric field E_p=+20 MV/m during t_p=10 min at T_p=353 K and measured after 1 day storage at room temperature The poled samples were illuminated with sine modulated IR radiation from the LED diode (0.96 μm, 5 mW) at the modulation frequency of 1 Hz–100 Hz.

3 Results and discussion

Figure 1 shows the dielectric responses of both investigated pure ceramics, which differ very much because of mixed contents of La^{3+}. The PLZT 9.5/65/35 ceramics exhibits two dielectric anomalies: the dispersive maximum at ~320 K and the low temperature anomaly at ~290 K. However, the dielectric spectrum of the PLZT 8/65/35 ceramic is characterized by the only one dielectric anomaly in the temperature range from 370 K to 410 K. The temperatures of ε' and ε'' maxima are shifted towards higher temperature region on increasing frequency. The permittivity maximum values ε' decrease, whereas the dielectric absorption maximum values ε''

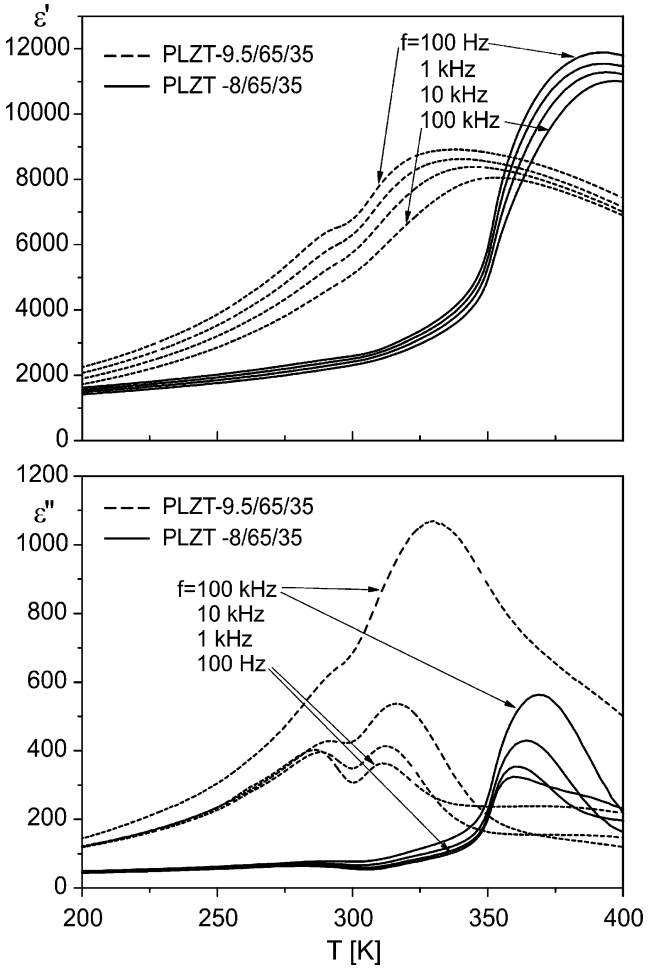

Fig. 1 Temperature dependence of real and imaginary part of the dielectric permittivity of the PLZT-*x*/65/35 ceramics with different content of lanthanum La^{3+} (*x*=8 – this work or 9.5 - [4])

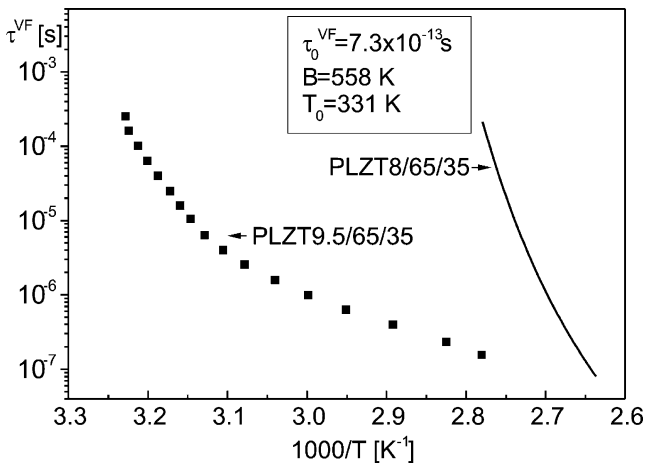

Fig. 2 Plots of relaxation time τ^{VF} as a function of reciprocal of the temperature related to the maximum of dielectric absorption for PLZT-*x*/65/35 ceramics with different content of lanthanum La^{3+} (*x*=8—this work or 9.5—[4])

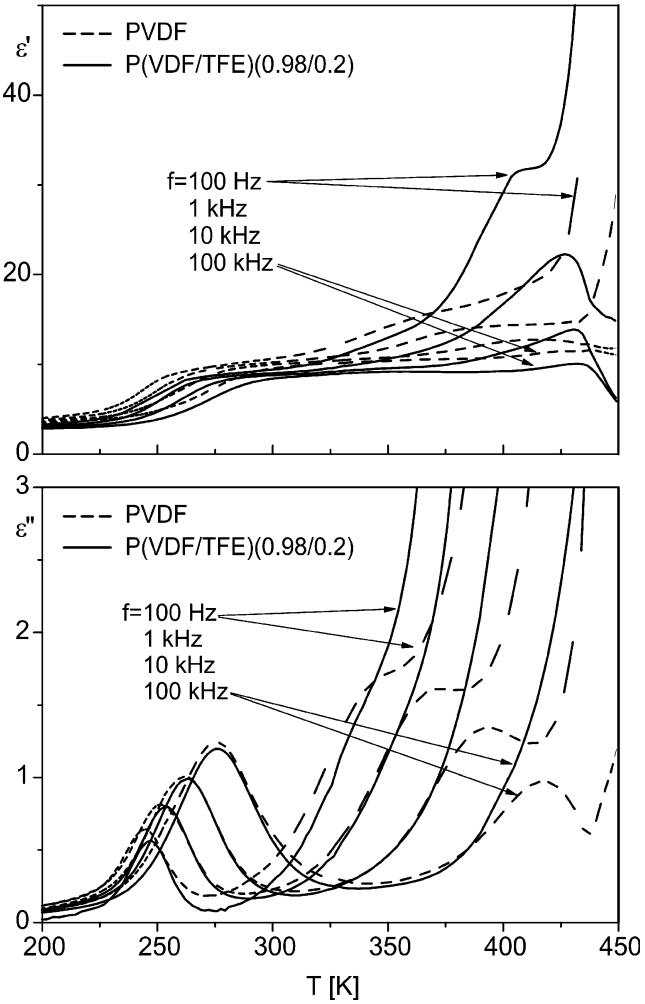

Fig. 3 Temperature dependence of real and imaginary part of the dielectric permittivity of the PVDF and P(VDF/TFE)(0.98/0.2)

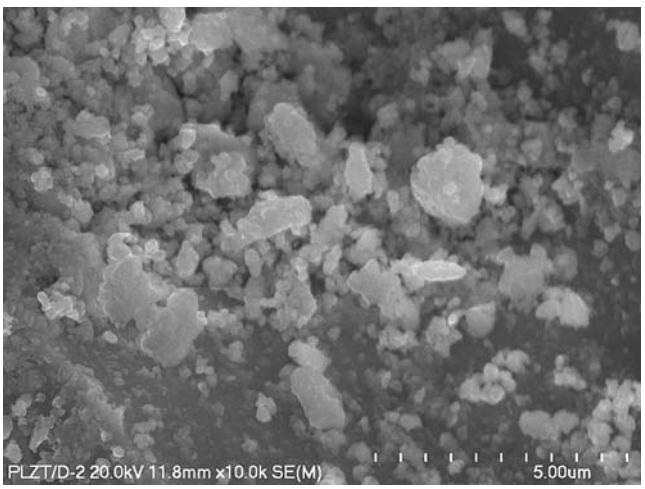

Fig. 4 SEM micrograph of PLZT 8/65/35 nanopowders after calcining (magnification ×10,000)

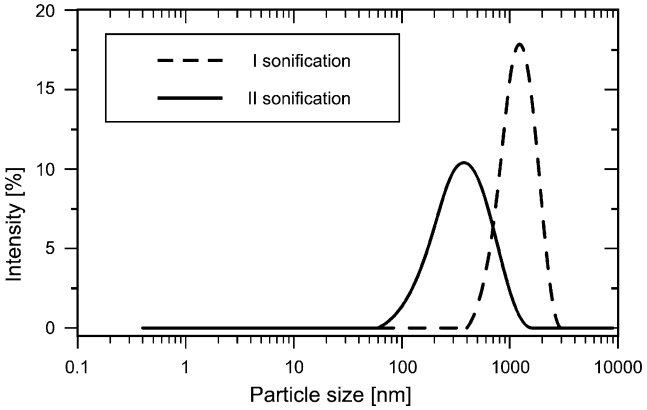

Fig. 5 Grain size distribution obtained by the DLS method

increase with increasing frequency. Such a dispersive behaviour of the dielectric permittivity is typical for ferroelectric relaxors [16] where the dynamics of polar nanoclusters is responsible for the dielectric response below the Burns temperature T_B (~620 K) [17–19]. Both dipole reversal (switching) of polar clusters and fluctuations of polar cluster boundaries contribute to the dielectric response below T_B [17]. Thus, our PLZT ceramics can be considered to be a ferroelectric relaxor.

Figure 2 shows the plots of relaxation time τ^{VF} as a function of reciprocal of the temperature related to the maximum of dielectric absorption for both pure ceramics. The plot obtained for the PLZT 8/65/35 ceramics obeys the Vogel–Fulcher law:

$$\tau^{VF}(T) = \tau_0^{VF} \exp[B/(T - T_0)]. \quad (1)$$

The continuous line results from the fitting of the experimental data to the Eq. 1. The parameters of the relaxation: pre-exponential factor τ_0^{VF}, activation energy B and the Vogel temperature T_0 are given on the graph. Our results are in a good agreement with those published by Bovtun et al. [17]. As the distribution of the relaxation times is determined by the size of the polar regions and the obtained results are located in the vicinity of the upper limit of the relaxation time determined for the PLZT 8/65/35 ceramics [17] it can be stated that the investigated ceramics is characterized by the large polar regions. The calculated Vogel–Fulcher temperature T_0=331 K corresponds very well with the freezing temperature T_f=328.5 K determined by Viehland et al. [19] from the temperature of the collapse in the remanent polarization. The plots of the relaxation time versus reciprocal of the temperature of the dielectric absorption maximum obtained for the PLZT 9.5/65/35 ceramics shows the deviation from the Vogel–Fulcher law. This results is very similar to that obtained by authors [19].

Dielectric dispersion and absorption of the P(VDF/TFE) (0.98/0.2) copolymer is shown in Fig. 3. To demonstrate the effect of the addition of tetrafluoroethylene on the dielectric spectrum of the copolymer, the proper temperature dependences obtained earlier by us [20] for the pure PVDF polymer are also inserted. One should notice three dielectric anomalies for both polymers. In the temperature range from 225 to 330 K the maxima of dielectric permittivity related to the glass transition are visible. A trace of relaxation related to wide-angle oscillation of polar groups followed by their rotation with main chain cooperation in the crystalline phase of the polymer is observed in the range 330–380 K [20]. The anomaly ascribed to the ferroelectric-paraelectric phase transition in the polymer appears at ~425 K. In the case of the P(VDF/TFE)(0.98/0.2) copolymer the relaxation pro-

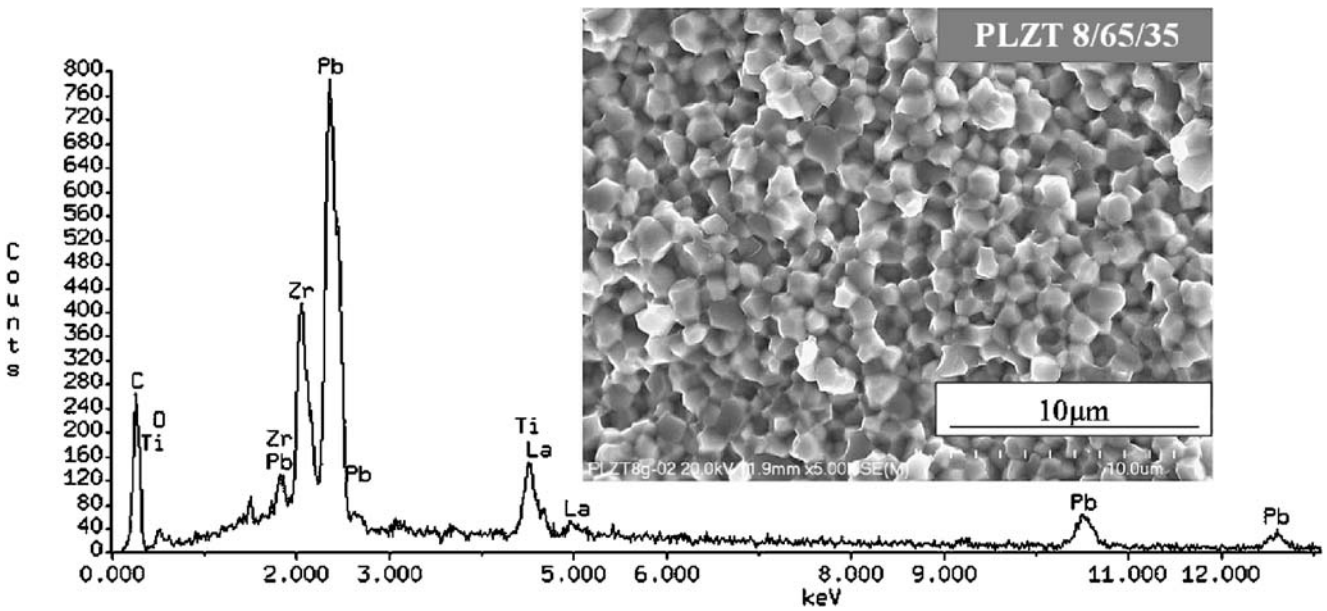

Fig. 6 EDS pattern and SEM micrograph of the fracture surface of sintered sample PLZT 8/65/35

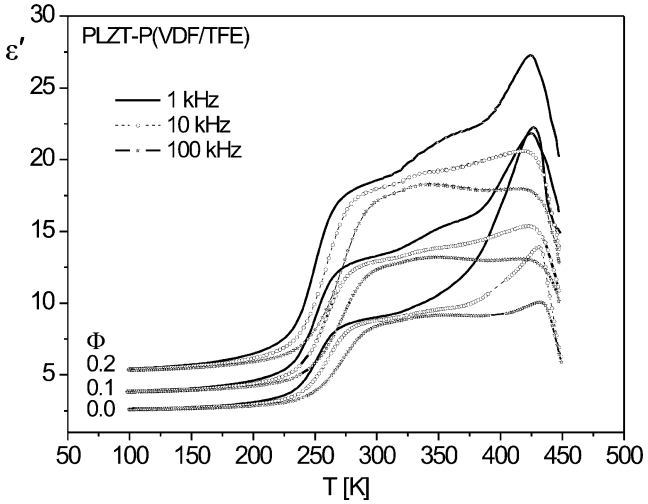

Fig. 7 Temperature dependence of dielectric permittivity ε' for the pure P(VDF/TFE) polymer and the PLZT-P(VDF/TFE) composites

cess created by the oscillation of the polar groups is hardly seen due to the electric conductivity of the TFE in the high temperature region. The combination of the PLZT ceramics and the P(VDF/TFE)(0.98/0.02) copolymer in a composite should result in new dielectric and pyroelectric properties, which are the subject of our study. The dielectric permittivity ε' and tgδ are involved in figures of merit (FOM) of various physical quantities and this is the reason for which the dielectric dispersion and dielectric loss measurements are necessary for design of materials for specific requirements.

Figure 4 presents the scanning electron microscopy (SEM) micrograph of the PLZT powders in which agglomerates of submicron particles can be observed. The agglomerates are typical for the other PLZT materials synthesized by the wet chemical route. They were disintegrated to the nanoscale grains during the sonification process, and after that the dynamic light scattering method (DLS) was used to estimate the grain size

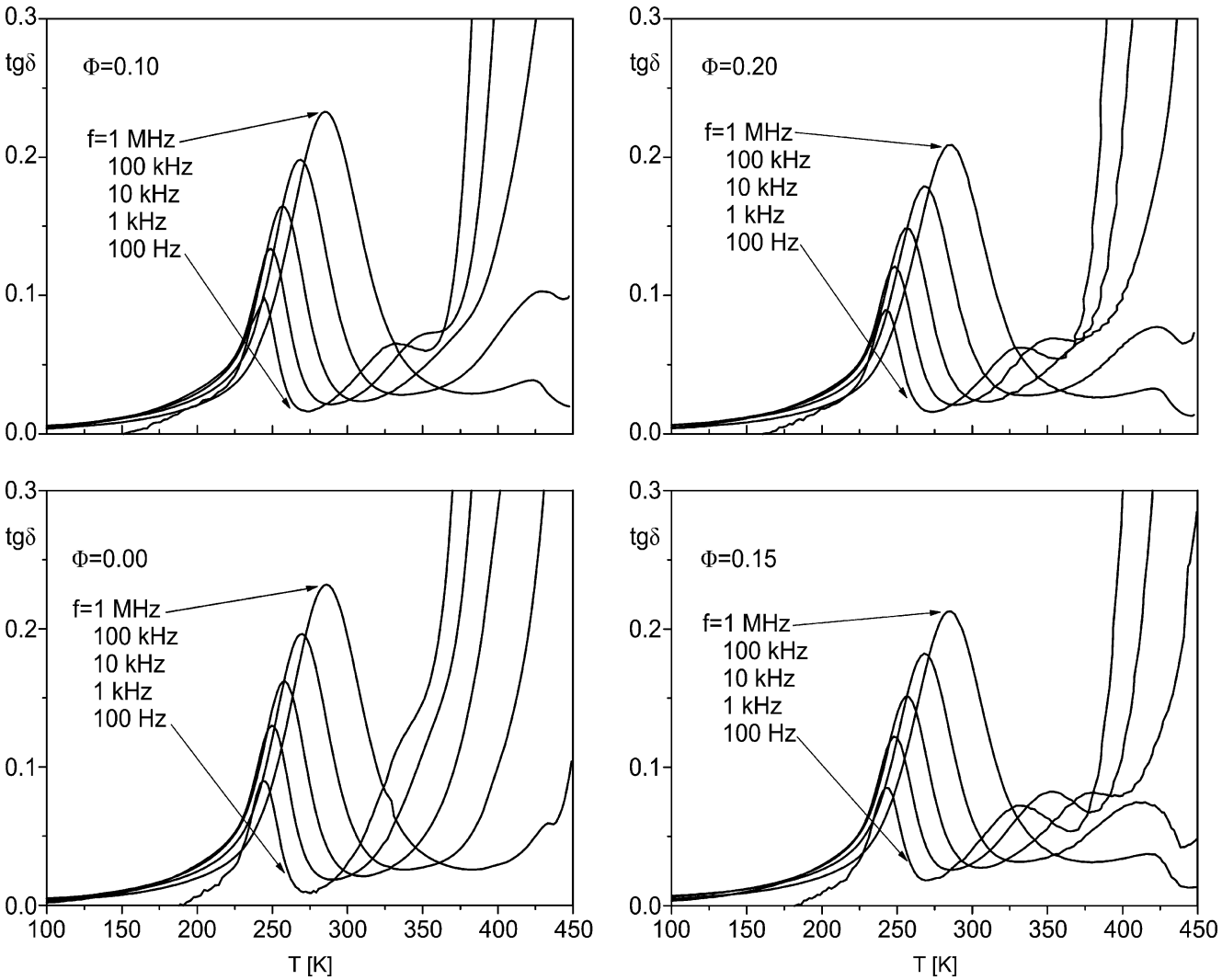

Fig. 8 Temperature dependencies of tgδ of polymer and the composites

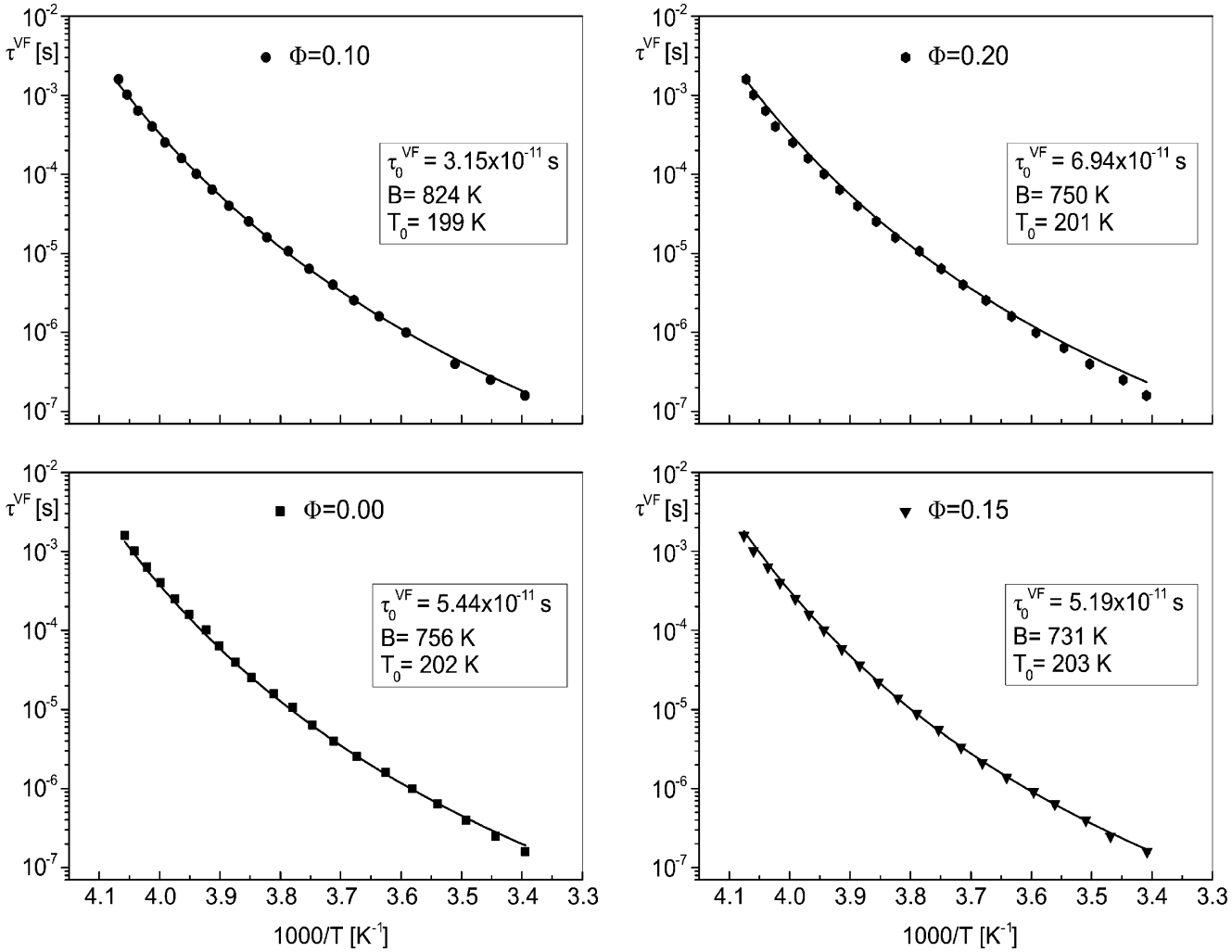

Fig. 9 Relaxation time τ^{VF} vs. reciprocal of the temperature ($1/T$) for pure P(VDF/TFE) polymer and the PLZT-P(VDF/TFE) composites

distribution. Small particles of nanometer size have still tendency to create larger agglomerates of the powders.

Figure 5 shows the grain size distribution obtained after I and II sonification. The analysis of PLZT powders after I sonification (t=0.5 h) gave the grain size distribution range of 400–3,000 nm. The measurement after II sonification (t= 0.5 h) brought the characteristic granularity in the range <1,000 nm with the mean value of the grain size amounting ~400 nm.

Ceramics samples were obtained by conventional sintering. The microstructure of the ceramics was investigated using a SEM. It was also used to carry out qualitative and quantitative tests of chemical composition (EDS) of powders and ceramics. The EDS patterns with SEM micrographs of the fracture surface of the ceramics are shown in Fig. 6. The EDS measurements confirm high purity (absence of doping elements) and homogeneity (uniform distributions of elements) of obtained materials [5, 10]. X-ray diffraction for PLZT powders confirms the crystal structure with rhombohedral symmetry. The crystal structure was identified as

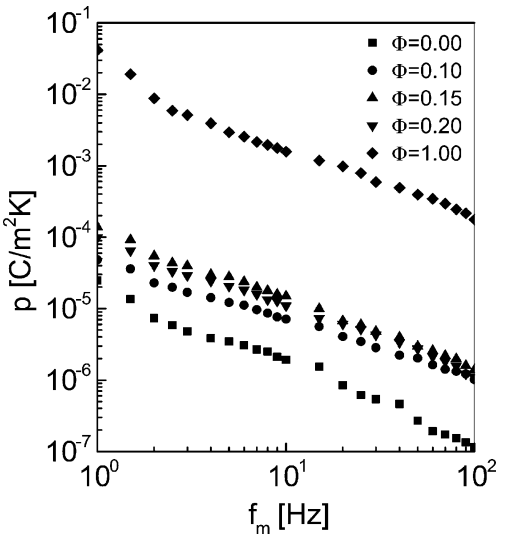

Fig. 10 Pyroelectric coefficient of pure P(VDF/TFE) polymer and PLZT-P(VDF/TFE) composites poled in E_p=20 MV/m at T_p=353 K vs. modulation frequency in comparison with that of the pure ceramics (Φ=1)

rhombohedral with the space group *R3m* and the parameters of the unit cell equal to a_h=0,5745 nm and c_h=0.7060 nm (the hexagonal setting was used for the indexing) [5].

The temperature dependencies of dielectric permittivity ε' for the pure P(VDF/TFE) polymer as well as the PLZT-P(VDF/TFE) composites with the volume fraction of the ceramics Φ=0.1 and 0.2 are presented in Fig. 7.

The addition of the PLZT ceramics increases the value of the dielectric permittivity ε' in the whole temperature range. It should be noticed that in the dielectric spectrum measured for the composites the maximum characteristic for the ceramics in the temperature range 350–400 K is also visible.

In Fig. 8 the temperature dependencies of tgδ of pure polymer P(VDF/TFE) and PLZT-P(VDF/TFE) composites are presented. The tgδ values of the composites are slightly lower than those of the polymer due to lower dielectric losses of the ceramics.

The addition of the ceramics causes also that the maxima ascribed to the wide-angle oscillation of polar groups (330–380 K) and to the ferroelectric-paraelectric phase transition (~425 K) in composites are more enhanced in comparison with the pure polymer. The maxima of tgδ in the temperature range 225–330 K are attributed to the α-relaxation process, related to the glass transition in the copolymer. The response observed for the composites is also determined by α-relaxation in P(VDF/TFE) polymer. Careful analysis of the α-relaxation in the composites allows to describe this process by the Vogel–Fulcher relationship (Eq. 1).

Figure 9 displays the dependence of the α-relaxation time τ^{VF} on the reciprocal of the temperature ($1/T$) for the pure polymer and the composites with the volume fraction Φ= 0.1, 0.15, 0.2. The points relate to the experimental data and the curves are obtained from fitting to the Vogel–Fulcher equation. The parameters of the α-process: pre-exponential factor τ_0^{VF}, activation energy B and the Vogel temperature T_0 resulting from fitting are given on each of the graphs. Because the values of the parameters are very similar, it can be stated that the addition of the PLZT ceramics to the P(VDF/TFE) polymer only slightly changes the dynamics of the glass transition in the polymer.

Figure 10 shows the pyroelectric response of the pure PLZT ceramics, pure P(VDF/TFE) polymer and the PLZT-P(VDF/TFE) composites after 1 day storage at room temperature. The contents of the ceramics improves the pyroelectric properties of the investigated samples. The pyroelectric coefficient p increases with the volume fraction Φ of the ceramics in the whole modulation frequency range (1–100 Hz). The values of the pyroelectric coefficient measured at 1, 10 and 100 Hz as well as the values of figures of merit $FOM_I = p/\varepsilon'$ (significant for sensor with high impedance amplifiers) and $FOM_{II} = p/(\varepsilon' \text{ tg}\delta)^{1/2}$ (important in the case when the noises of the sensor are mainly due to the pyroelectric element) are summarized in Table 1. It follows from the comparison that the values of the pyroelectric coefficient as well as FOM_I and FOM_{II} are considerably higher in the case of composites. However, further increasing the volume fraction Φ from 0.15 to 0.20 seems to reduce all these values. Moreover, it should be observed that the pyroelectric activity of the PLZT-P(VDF/TFE) composites is lower than that of the PLZT-P(VDF/TrFE) composites [4] due to much better pyroelectric coefficient and the figures of merit obtained for the copolymer P(VDF/TrFE) in comparison to the pure PVDF [21]. But nevertheless the pyroelectric response of the PLZT-P(VDF/TFE) composites was found to be several times higher than that of the PZT-PVDF composites because of higher activity of the copolymer P(VDF/TFE) in comparison with the polymer PVDF [21].

The pyroelectric coefficients measured for all investigated materials decrease with the modulation frequency. The increase of the pyroelectric activity of the composites due to addition of the ceramics is more predominant in the low frequency range. As follows from Fig. 10 and Table 1 the values of pyroelectric coefficient p as well as figures of merit vary very much with the volume fraction of the ceramics Φ at low frequencies (1 and 10 Hz). Whereas very little difference in coefficients is observed at the frequency 100 Hz. This behaviour we ascribe to the increase in the polarization in consequence of the presence of the polar molecules in the ceramics. The principle on which the pyroelectric effect is based concerns the charge generation associated with the spontaneous polarization change with the temperature [22]. The overall polarization of the composite, being the sum of three contributions: electronic, ionic and dipole reorientation-related, exhibits the maximum values at low frequencies and

Table 1 Pyroelectric coefficients p and figures of merit (FOM) of hot pressed polymer P(VDF/TFE) and PLZT-P(VDF/TFE) composites poled in field E_p=+ 20 MV/m during t_p=10 min at T_p=353 K after 1 day storage in room temperature for three modulation frequencies 1, 10 and 100 Hz.

Material	Volume fraction Φ	p (μC/m^{2}K)			FOM_I (μC/m^{2}K)			FOM_{II} (μC/m^{2}K)		
		1 Hz	10 Hz	100 Hz	1 Hz	10 Hz	100 Hz	1 Hz	10 Hz	100 Hz
Polymer	0.00	16.2	3.0	0.1	1.4	0.29	0.01	18.7	4.4	0.2
Composite	0.10	48.2	7.1	1.0	3.2	0.47	0.07	47.2	8.3	1.5
	0.15	139.2	14.9	1.4	7.0	0.82	0.08	109.5	14.2	1.6
	0.20	99.1	14.0	1.2	4.9	1.13	0.06	74.8	12.7	1.3

decreases with increasing frequency. The same behaviour shows the pyroelectric coefficient of the composites p [22].

4 Conclusions

The pyroelectric and dielectric response of hot-pressed PLZT-P(VDF/TFE) nanocomposites as a function of the volume fraction of the ceramics was investigated. The morphology, grain size distribution of PLZT 8/65/35 nanopowders and microstructure of the ceramics were also studied. The dielectric response of the composite was find to be the combination of those obtained for pure polymer and ceramics: the frequency dependence of dielectric permittivity is determined by the α-relaxation in P(VDF/TFE) polymer, attributed to the segmental molecular motion, and the dispersive maximum coming from the PLZT ceramics. The addition of the ceramics to the polymer matrix decreases dielectric losses in the composite. The results of the pyroelectric measurements indicated that the value of the ceramic volume fraction $\Phi \sim 0.15$ is the optimum which provides not only highest pyroelectric coefficient p but also the highest value of the figures of merit FOM_I and FOM_{II}. It is very important from the application point of view, i.e. when the pyroelectric sensors are used in devices of high electric impedance and low noises.

References

1. C.J. Dias, D.K. Das-Gupta, in *Electrets: Ferroelectric Ceramic/Polymer Composite Electrets*, vol. 2, ed. by R. Gerhard-Multhaupt (Laplacian, Morgan Hill, CA, 1999), p. 193
2. Y. Wang, W. Zhong, P. Zhang, J. Appl. Phys. **74**(1), 521 (1993). doi:10.1063/1.355263
3. F. Yang et al., J. Appl. Phys. **94**(4), 2553 (2003). doi:10.1063/1.1592292
4. B. Hilczer, J. Kułek, E. Markiewicz, M. Kosec, Ferroelectrics **293**, 253 (2003)
5. M. Olszowy, E. Markiewicz, C. Pawlaczyk, E. Nogas-Ćwikiel, M. Płońska, Paper presented at the XIII Int. seminar on physics and chemistry of solids, Ustroń, Pl, 10–13 June 2007
6. X. Tan, J.K. Shang, Scr. Mater. **43**, 925 (2000). doi:10.1016/S1359-6462(00)00514-5
7. G.H. Haertling, J. Am. Ceram. Soc. **82**, 797 (1999)
8. L.B. Kong, J. Ma, W. Zhu, O.K. Tan, Mater. Res. Bull. **36**, 1675 (2001). doi:10.1016/S0025-5408(01)00654-7
9. M. Cerqueira, R.S. Nasar, E.R. Leite, E. Longo, J.A. Varela, Ceram. Int. **26**, 231 (2000). doi:10.1016/S0272-8842(99)00047-4
10. M. Płońska, D. Czekaj, Z. Surowiak, Mater. Sci. **21**, 431 (2003)
11. N. Koizumi, J. Hagino, Y. Murata, Ferroelectrics **32**, 141 (1981)
12. H. Freimuth, C. Sinn, M. Dettenmaier, Polymer (Guildf.) **37**, 831 (1996). doi:10.1016/0032-3861(96)87261-2
13. Landolt-Börnstein, in *Science and Technology: Numerical Data and Functional Relationship*, Vol. III/28a (Springer, Berlin, 1981), p. 430
14. D. Viehland, Z. Xu, D.A. Payne, J. Appl. Phys. **74**, 7454 (1993). doi:10.1063/1.354968
15. A.G. Chynoweth, J. Appl. Phys. **27**, 78 (1956). doi:10.1063/1.1722201
16. L. Eric Cross, Ferroelectrics **151**, 305 (1994)
17. V. Bovtun, J. Petzelt, V. Porokhonsky, S. Kamba, Y. Yakimenko, J. Eur. Ceram. Soc. **21**, 1307 (2001). doi:10.1016/S0955-2219(01)00007-3
18. D. Viehland, Z. Xu, D.A. Payne, J. Appl. Phys. **74**, 7454 (1993). doi:10.1063/1.354968
19. D. Viehland, M. Wuttig, L.E. Cross, J. Appl. Phys. **69**, 6595 (1991). doi:10.1063/1.348871
20. B. Hilczer, J. Kułek, E. Markiewicz, M. Kosec, B. Malic, J. Non-Cryst. Solids **305**, 167 (2002). doi:10.1016/S0022-3093(02)01103-1
21. B. Hilczer, J. Kułek, E. Markiewicz, M. Kosec, Ferroelectrics **267**, 277 (2002)
22. K. Uchino, Ferroelectric Devices (Marcel Dekker, Basel, New York, 2000), pp. 2–3